JACS
JOURNAL OF THE AMERICAN CHEMICAL SOCIETY

ARTICLE

pubs.acs.org/JACS

Formation of C−C and C−O Bonds and Oxygen Removal in Reactions of Alkanediols, Alkanols, and Alkanals on Copper Catalysts

María E. Sad,[†,‡] Matthew Neurock,[§] and Enrique Iglesia*[,†]

[†]Department of Chemical Engineering, University of California at Berkeley, Berkeley, California 94720, United States

[‡]Catalysis Science and Engineering Research Group (GICIC), INCAPE (UNL-CONICET), Santiago del Estero 2654, (3000) Santa Fe, Argentina

[§]Departments of Chemical Engineering and Chemistry, University of Virginia, Charlottesville, Virginia 22904, United States

Supporting Information

ABSTRACT: This study reports evidence for catalytic deoxygenation of alkanols, alkanals, and alkanediols on dispersed Cu clusters with minimal use of external H_2 and with the concurrent formation of new C−C and C−O bonds. These catalysts selectively remove O-atoms from these oxygenates as CO or CO_2 through decarbonylation or decarboxylation routes, respectively, that use C-atoms present within reactants or as H_2O using H_2 added or formed *in situ* from CO/H_2O mixtures via water-gas shift. Cu catalysts fully convert 1,3-propanediol to equilibrated propanol−propanal intermediates that subsequently form larger oxygenates via aldol-type condensation and esterification routes without detectable involvement of the oxide supports. Propanal−propanol−H_2 equilibration is mediated by their chemisorption and interconversion at surfaces via C−H and O−H activation and propoxide intermediates. The kinetic effects of H_2, propanal, and propanol pressures on turnover rates, taken together with measured selectivities and the established chemical events for base-catalyzed condensation and esterification reactions, indicate that both reactions involve kinetically relevant bimolecular steps in which propoxide species, acting as the base, abstract the α-hydrogen in adsorbed propanal (condensation) or attack the electrophilic C-atom at its carbonyl group (esterification). These weakly held basic alkoxides render Cu surfaces able to mediate C−C and C−O formation reactions typically catalyzed by basic sites inherent in the catalyst, instead of provided by coadsorbed organic moieties. Turnover rates for condensation and esterification reactions decrease with increasing Cu dispersion, because low-coordination corner and edge atoms prevalent on small clusters stabilize adsorbed intermediates and increase the activation barriers for the bimolecular kinetically relevant steps required for both reactions.

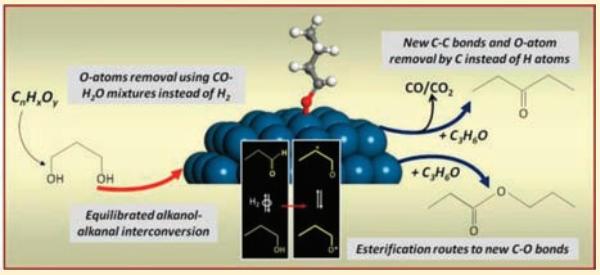

1. INTRODUCTION

Biomass-derived molecules typically contain excess oxygen that must be removed to render such species useful as fuels and chemicals.[1−3] Deoxygenation can proceed via elimination of H_2O or CO_2, in which the required H and C atoms are provided either by other molecules (e.g., H_2, CO) or by the reactants molecules themselves. The low H/C ratios prevalent in biomass-derived streams make hydrogen atoms a costly reactant for oxygen removal, irrespective of whether they are derived from the oxygenate molecules themselves (dehydration) or from external sources of H_2 (hydrodeoxygenation, HDO). Here, we examine alternate routes for oxygen removal, specifically those involving: (i) intramolecular use of carbon atoms through decarbonylation or decarboxylation reactions and (ii) hydrogenolysis or hydrogenation using hydrogen generated *in situ* via CO−H_2O reactions (water−gas shift), as potential alternatives to external sources of H_2. In doing so, we have recognized the high reactivity of Cu surfaces for the formation of new C−C and C−O bonds via condensation and esterification reactions.

Water-gas shift (WGS)[4] represents the simplest manifestation of selective removal of oxygen from an oxygenate (H_2O) using CO as the scavenger. CO/H_2O reactants have been used as reductants in hydrogenation reactions catalyzed by organometallic complexes,[5] such as the conversion of nitrobenzene to aniline, acetone to isopropanol, and benzaldehyde to phenol at high CO pressures in the liquid phase; such kinetic coupling between WGS and hydrogen addition reactions has not been reported, to our knowledge, on solid catalysts. Methanol and its mixtures with CO or CO−H_2O have been shown to form hydrogen-containing species that hydrogenate heavy oils using metal catalysts.[6] The *in situ* formation of H_2 from H_2O has been reported in carbohydrate reforming reactions, where the H_2 formed is then used to remove O-atoms from other oxygenates.[3,7−9] We provide evidence here for deoxygenation of alkanediols, alkanols and alkanals via hydrogen formed *in situ* in reactions of CO with H_2O on Cu catalysts, in pathways that combine the known properties of Cu catalysts in water−gas shift[10,11] and hydrogenation-dehydrogenation[12−15] reactions.

Received: August 24, 2011
Published: October 25, 2011

C−C formation reactions, such as aldol-type condensations, provide attractive routes to lengthen carbon chains and to decrease O/C ratios.[16−18] These reactions are typically catalyzed by acids and bases and involve reactions between alkanal and alkanol intermediates to form β-hydroxy carbonyl species that subsequently dehydrate to unsaturated alkanals or alkanones.[19] On solids, aldol-type condensations require dispersed basic oxides, such as MgO, Mg-AlO_x, ZnO, or alkali metal salts on silica.[20,21] Related Guerbet reactions convert primary alkanols to their β-alkylated dimers with concurrent loss of water at moderate temperatures (533−573 K) on several metal oxides (Cu, Zn, Cr, Mo, W, Mn).[22] These coupling reactions are thought to occur via alkanol oxidation to alkanals and their subsequent condensation to form α,β unsaturated alkanals that hydrogenate to alkanols in sequential reactions.[23] Cortright et al.[8] have reported C−C coupling reactions during aqueous phase reforming process on several metals supported on basic or acidic oxides. We show here that similar C−C coupling reactions are catalyzed by monofunctional Cu-based catalysts from gaseous reactants at low pressures without requiring the involvement of oxide supports. These catalysts also remove O-atoms as CO_x instead of H_2O, thus preserving scarce H-atoms within products.

Our results also confirm previously reported unique catalytic properties of Cu surfaces in esterification reactions[24] and provide evidence for mechanistic connections between esterification and condensation reactions. Chain lengthening involves aldol-type condensation and esterification reactions between adsorbed alkanals and basic alkoxide intermediates; these intermediates mediate the rapid equilibration between alkanals and alkanols on Cu clusters. Rates are controlled by reactions in which the alkoxide either acts as the base that abstracts the H-atom at the C_α position in adsorbed alkanals (condensation) or as the nucleophile that attacks the carbonyl group in adsorbed alkanals (esterification). The lower reactivity of small Cu clusters reflects their coordinatively unsaturated surfaces, which stabilize bound reactive intermediates, thus decreasing their reactivity in the kinetically relevant steps involved in these C−C and C−O bond formation reactions.

2. EXPERIMENTAL METHODS

2.1. Catalyst Synthesis. $Cu/ZnO/Al_2O_3$ (Cu/Zn/Al = 50/30/20) was prepared by coprecipitation from aqueous solutions (0.5 M) of $Cu(NO_3)\cdot 2.5H_2O$ (Aldrich, 99.99%), $Zn(NO_3)\cdot 6H_2O$ (Sigma-Aldrich, 98%) and $Al(NO_3)_3\cdot 9H_2O$ (Sigma-Aldrich, 98%) with a Na_2CO_3 solution (EMD Chemicals Inc. GR ACS) at 333 K in a stirred batch system. Mixed Cu, Zn and Al nitrate solutions were added dropwise to the stirred Na_2CO_3 solution (0.5 M). The resulting colloids were aged by stirring for 2 h at 333 K, separated by filtration, rinsed with deionized water at 330 K (0.5 L/g solid), and treated in ambient air at 373 K overnight. These precursors were decomposed in flowing dry He (Praxair, 99.99%, 0.83 $cm^3\ g^{-1}\ s^{-1}$) by heating to 673 K (at 0.033 K s^{-1}) and holding for 8 h. X-ray diffractograms of precursors detected hydrotalcite structures, which decomposed upon thermal treatment to form detectable CuO and ZnO phases (Supporting Information, Section S1). X-ray diffraction (XRD) patterns were measured using a Siemens D5000 diffractionmeter and Cu−Kα radiation (2θ = 5−80°; 2° min^{-1}). Cu-free ZnO-Al_2O_3 was prepared using the same procedure and Zn/Al ratio (ZnO/Al_2O_3; Zn/Al = 60/40, S_{BET} = 65 $m^2\ g^{-1}$) as for $Cu/ZnO/Al_2O_3$ to assess the reactivity of these oxides in alkanediol and alkanol reactions.

Cu clusters dispersed on carbon (HSAG 300, TIMREX, 230 $m^2\ g^{-1}$) and SiO_2 (CAB-O-SIL HS-5, 311 $m^2\ g^{-1}$) were prepared by their respective impregnations to incipient wetness with $Cu(NO_3)\cdot 2.5H_2O$ solutions. Several SiO_2-supported catalysts containing 5−20% wt. Cu were prepared by incipient wetness impregnation changing the temperature of thermal treatment (from 548 to 923 K) and using triethanolamine (Fluka, >98.5%) additives (Cu/triethanolamine molar ratio was 1:1) to vary Cu dispersion and cluster size.[25] These catalysts were treated in ambient air at 383 K for 12 h and then in flowing dry air (0.83 $cm^3\ g^{-1}\ s^{-1}$) by heating to 773 K (0.083 K s^{-1}) and holding for 5 h, unless other treatment protocols are specifically indicated. Samples were then cooled to ambient temperature and treated in flowing 10% H_2/He (Praxair, 99.999%, 5.56 $cm^3\ g^{-1}\ s^{-1}$) by heating to 553 K (at 0.167 K s^{-1}) and holding for 2 h and ultimately exposed to 1% O_2/He (Praxair, 99.999%, 0.83 $cm^3\ g^{-1}\ s^{-1}$) at ambient temperature for 1 h to passivate them before exposure to ambient air.

2.2. Surface Area, Metal Dispersion and Temperature-program Reduction Measurements. BET surface areas were measured using a Quantasorb 6 Surface Analyzer (Quantachrome Corp.) and N_2 at its normal boiling point after treating samples in 0.1 Pa dynamic vacuum at 473 K overnight. The Cu dispersion, defined as the ratio of surface $(Cu^0)_s$ to total Cu atoms, was determined by titration of surface Cu atoms with N_2O at 313 K using a stoichiometry of $N_2O/(Cu^0)_s$ of 0.5[26]

$$2Cu_s + N_2O \rightarrow Cu_s - O - Cu_s + N_2$$

on prereduced samples (0.3 g) treated in 20% H_2/Ar (Praxair, 99.999%, 5.6 $cm^3\ g^{-1}\ s^{-1}$) by heating to 553 K (at 0.167 K s^{-1}) and holding for 1 h. Samples were then flushed with Ar (Praxair, 99.999%, 5.6 $cm^3\ g^{-1}\ s^{-1}$) at 553 K for 0.5 h, cooled to 313 K, and exposed to flowing 0.5% N_2O/Ar (Praxair, 99.999%, 5.6 $cm^3\ g^{-1}\ s^{-1}$). N_2O uptakes were measured from the intensity of N_2O ions (44 amu) (Inficon, Transpector Mass Spectrometer) in the inlet and outlet streams. Mean Cu cluster diameters were estimated from Cu dispersions by assuming hemispherical clusters with the atomic density of bulk Cu.[27]

The reduction temperature of supported Cu catalysts was measured using temperature programmed reduction (TPR) methods. Samples (0.4 g, 125−180 μ) were placed within a quartz reactor, heated in Ar (Praxair, 99.999%, 5.6 $cm^3\ g^{-1}\ s^{-1}$) to 673 K ($Cu/ZnO/Al_2O_3$) or 773 K (Cu/SiO_2) at 0.33 K/s and held at this temperature for 0.5 h in order to remove H_2O before reduction. The samples were cooled to ambient temperature in Ar, the gas stream was switched to 20% H_2/Ar (0.67 $cm^3\ s^{-1}$, Matheson UHP, certified mixture) and the temperature was then increased to 1000 at 0.167 K s^{-1}. The effluent was analyzed by a quadrupole mass spectrometer (Inficon, Transpector Mass Spectrometer).

2.3. Catalytic Turnover Rates and Selectivities. Catalytic rates were measured with gas phase reactants at 503 K in a packed-bed with plug-flow hydrodynamics using prereduced and passivated catalysts (125−180 μm, 0.05−0.4 g) diluted with SiO_2 (125−180 μm aggregates, Fluka, purum. P.a., treated at ambient temperature with 0.5 M HNO_3 and treated in dry air at 673 K). All samples were treated again in 5% H_2/He (Praxair, 99.999%) at 533 K (0.0833 K s^{-1}) for 1 h before catalytic measurements. Liquid reactants (1,3-propanediol, Aldrich, 99.6%; propanol, Sigma-Aldrich, 99.7%; propanal, Acros, >99%; deionized water) were introduced using a syringe pump (Cole Parmer, 74900 series) by vaporizing each reactant into flowing He (Praxair, UHP) at 363 K (propanol, propanal), 378 K (water), or 433 K (1,3-propanediol). CO (Praxair, 99.999%) and H_2 (Praxair, 99.999%) were also used as reactants. Reactant and product concentrations were measured by gas chromatography (Agilent 6890) using a methyl silicone capillary column (Agilent, HP-1, 50 m, 0.32 mm ID, 1.05 μm film) connected to a flame ionization detector and a packed column (Porapak Q, 4.8 m, 1/8″ diameter, 80−100) connected to a thermal conductivity detector. Mass selective detection (HP 5972) after chromatographic separation (HP 5890 GC) was used for speciation of all reaction products.

Table 1. 1,3-Propanediol Conversion and Product Formation Rates and Selectivities on $Cu/ZnO/Al_2O_3$[a]

pressure [kPa]				selectivity[b] [%]			Formation rates [10^{-8} moles $g^{-1}s^{-1}$]		
H_2	CO	H_2O	conversion [%]	propene	propanal	propanol	propene	propanal	propanol
0	0	0	100	0.3	86	0.5	1.4	400	2
10	0	0	100	0.6	52	42	2.8	240	196
80	0	0	100	0.7	13	83	3.2	61	380
0	8	21	98	0.3	82	8	1.4	370	36
0	8	80	96	0.3	82	5	1.3	360	21
30	10	30	99	0.4	26	62	1.8	110	260

[a] 503 K, 216 g catalyst-ks (mol 1,3-propanediol)$^{-1}$ residence time, 0.8 kPa 1,3-propanediol, balance He, n.d.< 0.05%moles. [b] Carbons based selectivity, small amounts of acrolein, C_5 or C_6 also detected.

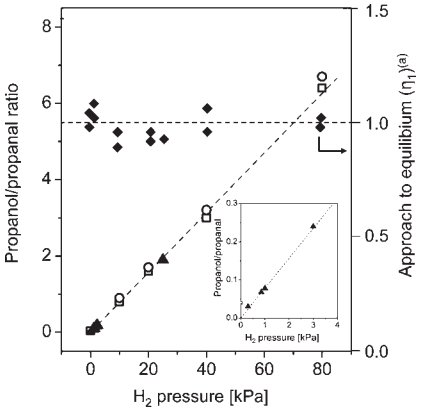

Figure 1. Effect of H_2 pressure (from added H_2 or H_2 formed in situ via water−gas shift) on propanol−propanal molar ratio during 1,3-propanediol reactions on $Cu/ZnO/Al_2O_3$. Alkanediol−H_2 reaction (□), alkanediol−H_2−CO reaction (○), alkanediol−CO−H_2O reaction (▲), approach to equilibrium for propanal−propanol−H_2 reaction (◆), - - - - equilibrium line. Propanol−propanal ratio for low H_2 pressures are shown in the small plot [216 g catalyst-ks (mol 1,3-propanediol)$^{-1}$ residence time, 503 K, 0.8 kPa 1,3-propanediol, balance He].

[a]Approach to equilibrium for propanal−propanol interconversion: $\eta_1 = [P_{propanol}]/[P_{H_2}] \times [P_{propanol}] \times 1/K^1_{eq}$, K^1_{eq}: equilibrium constant for propanal−propanol interconversion at 503 K.[28]

3. RESULTS AND DISCUSSION

3.1. 1,3-Propanediol Reactions with H_2 and CO−H_2O Coreactants. Table 1 shows conversion, selectivities, and rates for 1,3-propanediol reactions on $Cu/ZnO/Al_2O_3$ with and without added H_2 and CO−H_2O as coreactants. Products were not detected on SiO_2 (used as diluent) or in empty reactors; thus gas phase and SiO_2-mediated reactions do not occur at these conditions. ZnO/Al_2O_3 supports showed some propanediol conversion to acrolein, as discussed below.

1,3-Propanediol reactants were completely converted to equilibrated propanal−propanol mixtures (Figure 1, thermodynamic data[28]) and to trace amounts of other products on $Cu/ZnO/Al_2O_3$, even without H_2 coreactants (Table 1, first row). Propanal−propanol equilibriation was confirmed at all conditions from approach to equilibrium parameters (η_1, defined in Figure 1) that were unity within experimental accuracy (Figure 1). Propene, allyl alcohol (2-propen-1-ol), acrolein (2-propenal) and C_5−C_6 oxygenates were also detected at low concentrations in the effluent stream. Propanal was the predominant product in the absence of added H_2 (86% selectivity) and small amounts of acrolein were also formed, consistent with thermodynamic expectations.[28]

Scheme 1. Reaction Network for 1,3-Propanediol Deoxygenation

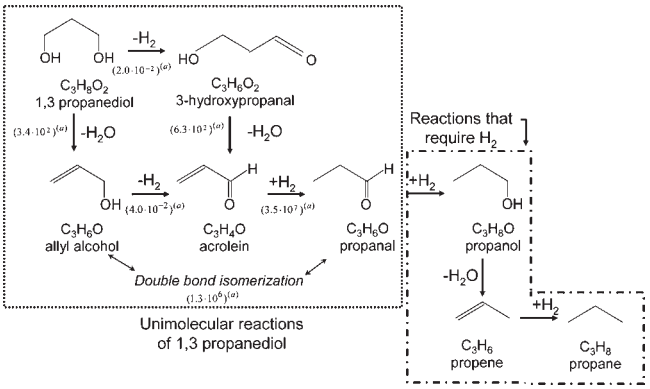

[a] Equilibrium constants calculated at 503 K,[28] thermodynamic properties of 3-hydroxy-propanal were estimated by group contribution method in Aspen v7.1

These products are consistent with the 1,3-propanediol conversion pathways shown in Scheme 1, in which allyl alcohol forms initially (thermodynamically favored, $K_{eq} = 3.4 \times 10^2$ bar at 503 K[28]) and then undergoes dehydrogenation to produce acrolein with unfavorable thermodynamics ($K_{eq} = 0.04$ bar at 503 K[28]). The double-bond isomerization of allyl alcohol to propanal occurs rapidly via intramolecular or intermolecular hydrogen transfer and is favored by thermodynamics ($K_{eq} = 1.2 \times 10^6$ at 503 K[28]). Fast hydrogenation steps then form propanol in amounts dictated by thermodynamics at the prevalent H_2 pressures. Propene and propane can also form via dehydration and hydrogenation reactions, but usually require acid sites; propane was not detected with propanediol−H_2 reactants and propene selectivities were very small (<1%, Table 1). 1,3-Propanediol forms propanal on Cu/Al_2O_3 at 523 K[29] via pathways proposed to involve 3-hydroxypropanal dehydration to acrolein and subsequent hydrogenation. As a result, Scheme 1 also includes this route. The prevalent equilibration among these products in these experiments precludes more specific conclusions about the actual routes involved in the equilibration of propanediol reactants with propanol−propanal products.

H_2-propanediol reactant mixtures predominantly formed equilibrated propanal−propanol mixtures with traces of allyl

alcohol, acrolein, propene, and C_5-C_6 oxygenates (Table 1). Propanol−propanal ratios were proportional to H_2 pressures and their values were accurately described by the thermodynamics of their interconversion[28] (10−80 kPa H_2, Figure 1). Propane was not detected among reaction products, even at residence times that equilibrated propanol and propanal products, indicating that propanol hydrogenolysis and propene hydrogenation do not occur at detectable rates at these conditions.[24,30,31]

Figure 2 shows conversions and product yields (moles of C in *i* product per mole of C in 1,3-propanediol in the feed) as a function of residence time for reactions of 1,3-propanediol with H_2 (10 kPa) as coreactant. The equilibrated nature of propanal−propanol interconversions allow us to consider these two molecules as a kinetically indistinguishable chemical lump, denoted hereinafter as the reactant pool. The nonzero initial slopes for propanal−propanol and acrolein yields (Figure 2) indicate that they form either directly from propanediol or via sequential routes mediated by reactive intermediates present at trace concentrations (e.g., allyl alcohol or 3-hydroxypropanal). Acrolein yields increased with residence time and then decreased, consistent with the involvement of acrolein as an intermediate in the formation of propanol and propanal. Propene yields show a zero initial slope, consistent with its formation via slow reactions of equilibrated propanol−propanal mixtures and not directly from propanediol (Scheme 1).

The possible involvement of the support in 1,3-propanediol conversion was examined by comparing rates with 1,3-propanediol−H_2 and 1,3-propanediol−He on $Cu/ZnO/Al_2O_3$ and ZnO/Al_2O_3 (Table 2). 1,3-Propanediol conversion rates were much larger on $Cu/ZnO/Al_2O_3$ than on ZnO/Al_2O_3 (40 and 60 times, with and without H_2) (Table 2); these effects of Cu are even stronger than indicated by these data when we consider the smaller kinetic driving force imposed by the higher conversions prevalent on the $Cu/ZnO/Al_2O_3$ sample. Acrolein was the main product on ZnO/Al_2O_3 without added H_2 and acrolein and propanal were not in equilibrium on $Cu/ZnO/Al_2O_3$ or ZnO/Al_2O_3 at any H_2 pressure. On $Cu/ZnO/Al_2O_3$, the approach to equilibrium parameter (η_2, defined in Table 2) was ∼10, indicating that propanal did not form from acrolein; we conclude that propanal forms via either isomerization of allyl alcohol or hydrogenation of bound acrolein species before their desorption. On ZnO/Al_2O_3, the acrolein-propanal approach to equilibrium factor was 0.1−0.3 (Table 2), suggesting that propanal forms slowly from allyl alcohol or acrolein and that acrolein is the initial product of propanediol reactions in the absence of Cu. The approach to equilibrium values for propanal−propanol−H_2 reactions (η_1) were near unity on $Cu/ZnO/Al_2O_3$ but larger than unity on ZnO/Al_2O_3 (Table 2), consistent with hydrogenation of propanal to propanol on Cu sites and with propanal as an "earlier" product of propanediol reactions than propanol on ZnO/Al_2O_3 catalysts. The presence of H_2 (10 kPa) did not influence diol conversion rates on $Cu/ZnO/Al_2O_3$ (Table 2), but increased diol conversion rates on ZnO/Al_2O_3 (Table 2) by hydrogenating acrolein to propanal and overcoming, in this manner, the thermodynamic constraints associated with acrolein formation. We conclude that ZnO/Al_2O_3 supports catalyze 1,3-propanediol dehydration-dehydrogenation to acrolein, but that sequential acrolein hydrogenation to propanal and propanol and hydrogen transfer isomerization of allyl alcohol to propanal occur slowly in the absence of Cu. In the presence of Cu, propanal forms rapidly via diol dehydration to allyl alcohol and subsequent hydrogen transfer reactions to form equilibrated propanal−propanol mixtures.

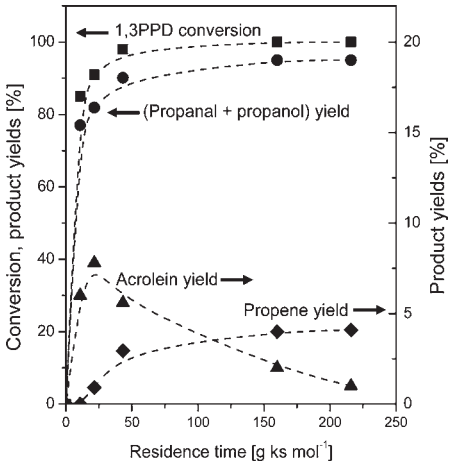

Figure 2. Effect of residence time on 1,3-propanediol conversion and product yields on $Cu/ZnO/Al_2O_3$ (503 K, 0.8 kPa 1,3-propanediol, 10 kPa H_2, balance He).

Table 1 shows the effects of the H_2 molecules formed *in situ* via water−gas shift when CO−H_2O mixtures were introduced together with 1,3-propanediol on $Cu/ZnO/Al_2O_3$. WGS rates without diol coreactants are shown in Table 3. CO conversions decreased with time on stream from 24% (0.9 ks) to 4% (after 10.8 ks) with 21 kPa H_2O at 503 K (and from 60 to 15% with 80 kPa H_2O); deactivation was not observed, even after 25 ks, however, when H_2 (30 kPa) was added with CO/H_2O reactants (Table 3), as also shown in previous studies.[32] H_2 was added to all reactant streams containing CO and H_2O to prevent deactivation processes that would otherwise interfere with accurate rate and selectivity measurements. H_2 effluent concentrations decreased when 1,3-propanediol (0.8 kPa) was added to CO−H_2O

Table 2. Effect of Support on 1,3-Propanediol Conversion and Product Formation Rates and Selectivities on $Cu/ZnO/Al_2O_3$[a]

					carbon-based selectivity [%]			product formation rates[d] [10^{-8} moles g^{-1} s^{-1}]			
catalyst	H_2 [kPa]	conversion [%]	η_1[b]	η_2[c]	acrolein	propanal	propanol	acrolein	propanal	propanol	sum
$Cu/ZnO/Al_2O_3$[e]	0	80	0.95	10	25	70	2	1900	5200	150	7200
$Cu/ZnO/Al_2O_3$[e]	10	85	1.1	9	2	50	37	160	3900	2900	7000
ZnO/Al_2O_3[f]	0	25	0.2	0.1	84	11	n.d.	97	13	n.d.	110
ZnO/Al_2O_3[f]	10	40	0.4	0.3	41	36	5	76	67	9	150

[a] 503 K, 0.8 kPa 1,3-propanediol, balance He; n.d.< 0.05%moles. [b] Approach to equilibrium for propanal−propanol−H_2 reaction defined in Figure 1. [c] Approach to equilibrium for acrolein-propanal−H_2 reaction $\eta_2 = [P_{propanol}]/[P_{H_2}] \times [P_{acrolein}] \times 1/K_{eq}^2$. [d] Integral rates, calculated by dividing the 1,3-propanediol fractional conversion by the residence time. [e] 10.8 g ks mol^{-1} residence time. [f] 216 g ks mol^{-1} residence time.

dx.doi.org/10.1021/ja207551f | J. Am. Chem. Soc. 2011, 133, 20384–20398

Table 3. H_2 Formation Rates during CO−H_2O Reactions on Cu/ZnO/Al_2O_3 in the Presence or Absence of 1,3-Propanediol Coreactants[a]

pressure[b] [kPa]				CO conversion[c] [%]		net H_2 formation rate[d] [10^{-6} moles g^{-1} s^{-1}]		H_2 consumption rate[e] [10^{-6} moles g^{-1} s^{-1}]	
				time on stream [ks]		time on stream [ks]		time on stream [ks]	
CO	H_2O	H_2	1,3-PPD	0.9	10.8	0.9	10.8	0.9	10.8
8	21	0	0	24	4.0	12	2.1	-	-
8	80	0	0	60	15	34	7.6	-	-
10	30	30	0	65[f]	65	10	10	-	-
8	21	0	0.8	12	3.7	6.3	1.9	0.026	0.019
8	80	0	0.8	37	9.9	19	5.1	0.020	0.012
10	30	30	0.8	46[f]	46	7.1	7.0	0.021	0.020

[a] 503 K, 19.7 g ks mol CO^{-1} residence time, balance He. [b] Reactor inlet pressure. [c] CO conversion calculated as (moles CO^{out}-moles CO^{in})/mols CO^{in}. [d] Calculated as: moles H_2 produced/residence time expressed as g catalyst-g (moles CO^{in}). [e] Calculated as: moles propanol produced from 1,3PPD/residence time expressed as g catalyst-g (moles 1,3-PPD^{in}). Propanol was used because it was the only product that consumes H_2 (1 mol of H_2 is necessary to produce 1 mol of propanol) produced from the alkanediol. [f] 64.9 g catalyst-ks (mol CO)$^{-1}$ residence time.

Scheme 2. Reactions Steps Involved in Propanol−Propanal Equilibration and C−C and C−O Coupling Reactions from C_3 Intermediates on Cu Catalysts

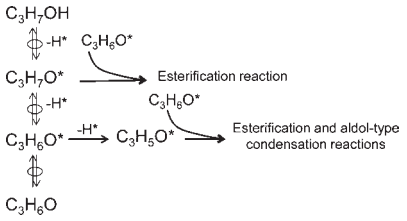

inlet streams, either because of WGS inhibition by diols or H_2 depletion by conversion of 1,3-propanediol to propanol. H_2 consumption rates via the latter route were much smaller than the decrease in H_2 effluent molar rates observed upon diol addition (Table 3), indicating that 1,3-propanediol (or propanol−propanal products) inhibits WGS reactions, possibly via competitive adsorption or reactions with CO and H_2O.

1,3-Propanediol conversions and selectivities with CO/H_2O and CO/H_2O/H_2 coreactants are shown in Table 1. Diol conversions were >95% and equilibrated propanol−propanal mixtures were the main products. Propanol−propanal interconversion involves the formation of adsorbed alkoxides, via O−H activation in alkanols or H-addition to alkanals,[33] in steps that are fast and quasi-equilibrated at all experimental conditions. Scheme 2 shows that ROH species can undergo O−H activation on Cu surfaces to form alkoxides. These alkoxides can then dehydrogenate to form alkanals (as shown by propanol−propanal equilibration). These adsorbed alkanals can subsequently react with vicinal alkoxides or $C_3H_5O^*$ species formed via alkanal dehydrogenation, mediated by bound alkoxides to form C−O or C−C bonds via bimolecular esterification or condensation reactions, respectively (as discussed in section 3.2.1). The $C_3H_5O^*$ nomenclature is used to indicate that while the key surface intermediates for both esterification and condensation contain the same atomic composition, their atomic structures can be different. The low alkane selectivities observed in alkanol−H_2 or alkanediol−H_2 reactions indicate that Cu does not activate the C−O bonds in these oxygenates before formation of new C−C or C−O bonds and that hydrogenolysis of these oxygenates therefore does not occur.

We conclude from these data that 1,3-propanediol is completely converted to equilibrated propanol−propanal mixtures even at short residence times and modest temperatures (∼500 K) on Cu/ZnO/Al_2O_3 (Table 1). The fast nature of the 1,3-propanediol dehydration and hydrogenation-dehydrogenation on all Cu catalysts tested (also on Cu/SiO_2 catalysts, data not shown) preclude a more rigorous kinetic and mechanistic analysis of these reactions. The rapid formation of equilibrated propanal−propanol led us to examine the identity and mechanism of subsequent reactions of these molecules at longer residence times in the presence of H_2, CO, H_2O and mixtures thereof.

3.2. Catalytic Reactions of Propanol and Propanal on Cu-based Catalysts. In a later section (3.2.2), we show that supports do not influence rates and selectivities in reactions of propanal−propanol−H_2 mixtures. In view of this, we focus here on Cu/SiO_2 catalysts, which can be prepared with a wide range of mean Cu cluster sizes, in our kinetic and mechanistic studies. As in the case of 1,3-propanediol, propanol, propanal, and their mixtures equilibrated rapidly at all H_2 pressures (Figure 3, line denotes equilibrium ratios[28]) and also when H_2 was formed *in situ* via CO/H_2O reactions (Figure 3). As stated earlier, propanol and propanal can be rigorously treated as a single chemical species (reactant pool) and conversions and selectivities are based on the inlet and outlet molar rates of these combined reactants.

3.2.1. Primary and Secondary Products in Propanol−Propanal−H_2 Reactions on Cu Catalysts. Equilibrated propanol−propanal−H_2 mixtures formed a broad range of products on 5% wt. Cu/SiO_2 catalyst (5.6% dispersion; 0.64 kPa propanol, 80 kPa H_2; Figure 4) at residence times (2160 g-ks/(mol propanol)$^{-1}$) significantly larger than those required to form these equilibrated mixtures from 1,3-propanediol (216 g-ks/(mol 1,3-propanediol)$^{-1}$). These products include oxygenates, predominantly 3-pentanone and propyl propionate, with 2-methylpentanal and 2-methyl-3-pentanone as minority species. Propene and propane were detected in small concentrations and propane/propene molar ratios were smaller than predicted from their interconversion equilibrium (∼ 0.1, K_{eq} = 1.3•10^6 at 503K[28]), suggesting that small amounts of propene formed via dehydration of propanol undergo slow secondary hydrogenation-dehydration on Cu.[34] The trace amounts of 3-pentanol detected correspond to its unfavorable equilibrium with 3-pentanone (K_{eq} = 3.6•10^{-3} bar^{-1} at 503K[28]), as also found for the other C_6 alkanals and alkanones and their respective alkanols.

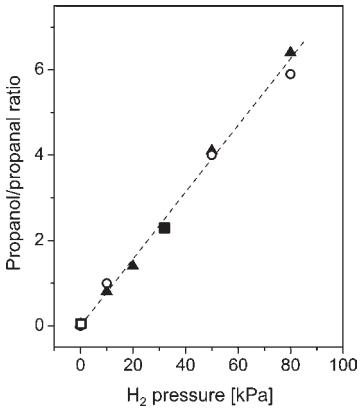

Figure 3. Effect of H_2 pressure (from added H_2 or H_2 formed *in situ* via water−gas shift) over propanol−propanal molar ratio during propanol−H_2 or propanal−H_2 reactions on $Cu/ZnO/Al_2O_3$. Propanol−H_2 (▲), propanal−H_2 (○), propanol−CO−H_2O reaction: 21 kPa H_2O, 8 kPa CO (■), 30 kPa H_2O, 30 kPa H_2, 10 kPa CO (□), - - - propanol−propanal equilibrium line [503 K, 2160 g catalyst-ks (mol 1,3-propanediol)$^{-1}$ residence time, 0.64 kPa propanol or propanal, balance He].

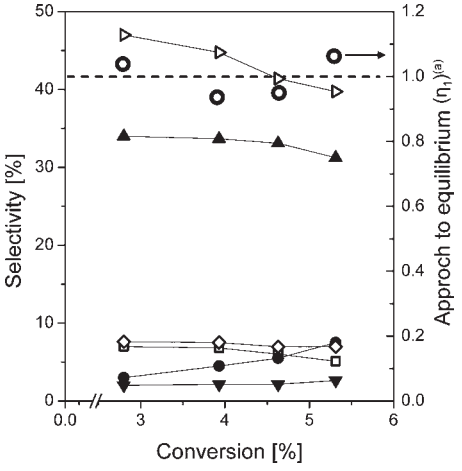

Figure 4. Selectivity[b] vs conversion[c] for propanol−propanal−H_2 reactions and approach to equilibrium for propanol to propanal transformation (η_1) on 5 wt % Cu/SiO_2. Selectivities to propane (●), propene (□), 3-pentanone (▷), propyl propionate (▲), 2- methyl-3-pentanone (◇), 2-methyl pentanal (▼) and approach to equilibrium for propanol to propanal and H_2 reaction, η_1 (○) [5% wt. Cu/SiO_2, 5.6% dispersion, 503 K, 2160 g catalyst-ks (mol propanol)$^{-1}$, 0.64 kPa propanol, 80 kPa H_2, balance He].

[a]Approach to equilibrium for propanal−propanol interconversion defined in Figure 1.

[b]Defined as: $S_i = (F_i^{out})/(F^{in}_{propanal} - F^{out}_{propanal\ +\ propanal})$ where F_j are the molar rates.

[c]Defined as: $X = (F^{in}_{propanol} - F^{out}_{propanal\ +\ propanal})/(F^{in}_{propanal})$ where F_j are the molar rates.

The effects of residence time (and pool conversion) on selectivities were used to probe the primary or secondary nature of all products formed (Figure 4). The approach to equilibrium (η_1) for propanol/propanal interconversion was near unity at all conversions and residence times. 3-Pentanone, propyl propionate, 2-methyl pentanal, 2-methyl 3-pentanone and propene selectivities gave nonzero values when extrapolated to zero

Scheme 3. Reaction Network for Propanol−Propanal Reactions on Cu-based Catalyst

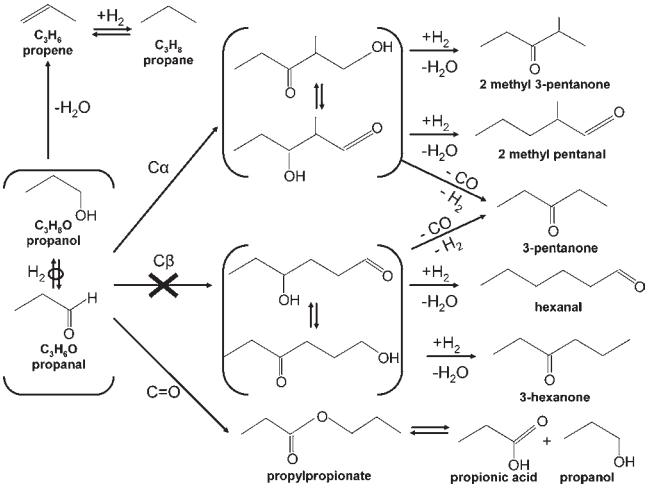

conversion, consistent with their direct formation as primary products from the propanal−propanol reactant pool; propane gave zero initial slope, as expected from its formation via secondary hydrogenation of propene derived from propanol dehydration instead of via primary hydrogenolysis reactions of propanol.

Equilibrated propanal−propanol−H_2 mixtures preferentially formed C_5 and C_6 molecules with fewer O-atoms via condensation and esterification reactions but only small amounts of deoxygenated C_3 molecules. The formation of each product is described schematically in Scheme 3 as four general types of reactions from equilibrated propanol−propanal mixtures:

(i) aldol-type condensation reactions[20] by activation of C−H bonds at α-positions to form an aldol intermediate that can further react to 2-methyl-3-pentanone and 2-methyl-pentanal or undergo decarbonylation or decarboxylation to form 3-pentanone

(ii) formation of linear C_6 alkanals and alkanones by activation of C−H bonds at β-positions

(iii) esterification reactions to form propyl propionate[35]

(iv) dehydration of propanol to propene and subsequent hydrogenation

Base-catalyzed aldol condensation involves reactions of carbonyl species with enolate intermediates of another carbonyl species to form β-hydroxy carbonyl compounds (aldols), which subsequently dehydrate to α,β-unsaturated carbonyls and hydrogenate to the corresponding alkanal or alkanone.[19,36] On bases, low hydrogenation rates (or the absence of H_2) lead to α,β-unsaturated species and condensation occurs only for carbonyl species that contain an α-H atom. For example, propanal reactions on Mg/Al oxides form aldols as primary products; these species undergo fast dehydration-hydrogenation or hydrogenolysis to form 2-methyl 3-pentanone and 2-methyl-pentanal.

Cu-based catalysts form 2-methyl-pentanal and 2-methyl-3-pentanone (Figure 4, Scheme 3), the expected products of aldol-type condensation reactions of propanal−propanol mixtures, but 3-pentanone is the predominant product, apparently as a result of decarbonylation or decarboxylation (instead of dehydration) of aldol-type intermediates, in contrast with the data reported for Cu supported on basic solids,[31] for which C_6 alkanones are the

main products. Aldol-type reactions of alkanols are known as Guerbet reactions[37] and occur on oxides of Cu, Zn, Cr, Mo, W, and Mn[21] with loss of oxygen as H_2O instead of CO_x. 1-Alkanols with *n*-carbons react on $Cu/ZnO/Al_2O_3$ to form esters with $2n$ carbons and alkanones with $2n$ or $2n - 1$ carbons ($2n - 1$ alkanones form by CO_x loss) via steps that are thought to involve aldol-type species formed via recombinative desorption of the H-atoms that result from C−H activation steps on basic support sites on Cu surfaces,[30] as also proposed on Cr oxide catalysts.[38] These studies have implicated the essential involvement of support basic sites in C−C bond formation. We show in the present paper (section 3.2.2.), however, that monofunctional Cu surfaces catalyze aldol-type C−C coupling reactions and the removal of O-atoms using C-atoms within oxygenate molecules without any detectable assistance by the support.

Esters are typically formed via reactions of organic acids with alkanols using acid catalysts[19] but can also form from alkanals lacking an α-hydrogen via Tishchenko or Cannizaro reactions using bases as catalysts. The Tishchenko route[35,39] involves reactions of alkanals with alkoxide species, while the Cannizaro reaction[40] involves the reduction of an alkanal species to the alkanol, the oxidation of another alkanal molecule to carboxylic acid, and their subsequent bimolecular reactions. Another route proposed for ester formation involves hemiacetal intermediates formed via reactions between alkanals and alkanols on $CuO/ZnO/Al_2O_3$.[24,31]

Next, we provide evidence that condensation and esterification proceed via monofunctional routes on Cu/SiO_2 (Figure 4) and that metallic Cu cluster surfaces stabilize all intermediates required to equilibrate alkanal-alkanol mixtures and to mediate their C−C and C−O formation reactions without assistance by SiO_2 supports. Cu clusters dissociate O−H bonds in alkanols to form surface alkoxides[33] that dehydrogenate to alkanals in the steps shown in Scheme 2. Adsorbed alkoxides also act as bases in reactions with alkanals via the two routes also shown in Scheme 2. In one route, alkoxides abstract the acidic α-hydrogen in adsorbed alkanals to form adsorbed enolate species that ultimately attack the electrophilic carbonyl group in a vicinal alkanal to form a new C−C bond in aldol-type condensation steps. The basic O-atom in adsorbed alkoxides can also attack the electrophilic carbonyl group in a vicinal alkanal to form a new C−O bond and the esterification products. Linear alkanal (hexanal, 3-hexanone) or alkanol products were not detected, indicating that C−H bonds at β-positions are unreactive, as typically observed in aldol condensations by acids or bases.[36] We discuss both of these paths in more detail below in the specific context of the kinetic response of condensation and esterification reactions to the concentrations of propanal, propanol, and H_2.

3.2.2. Effects of Support in Propanol−Propanal−H_2 Reactions on Cu. Figure 5 shows the selectivity to the various products formed from propanol−propanal−H_2 reactants on Cu clusters supported on SiO_2, carbon, and ZnO/Al_2O_3 at similar reactant pool conversions (~5−7%). All catalysts predominantly formed propyl propionate and 3-pentanone. Additional SiO_2 (0.3 g), present as a physical mixture with 20% wt. Cu/SiO_2 (0.05 g), did not influence rates or selectivities. We conclude from the prevalence of esterification and condensation products on all Cu clusters, irrespective of the amount or identity of the support that condensation and esterification, occur via monofunctional Cu-catalyzed pathways. Although it has been reported that esterification can occur on Cu surfaces,[21] the ability

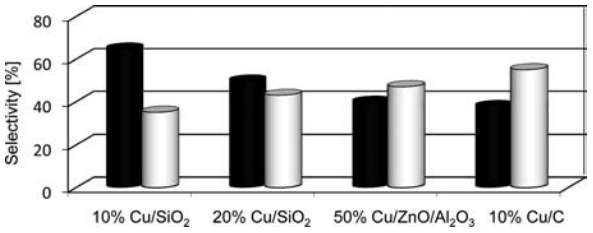

Figure 5. Products selectivity (defined in Figure 4) for propanol/propanal/H_2 reaction on Cu supported catalysts (pool conversion = 5−7%). Selectivity to 3-pentanone (black) and propyl propionate (gray). 503 K, 0.64 kPa propanol, 10 kPa H_2, balance He, 2700 g-ks (mol propanol)$^{-1}$ residence time for 10% wt. Cu/SiO_2, 20% wt. Cu/SiO_2 and 10% wt. Cu/C, 540 g-ks (mol propanol)$^{-1}$ residence time for 50% wt. $Cu/ZnO/Al_2O_3$.

of Cu metal surfaces to catalyze condensation reactions by activating the C−H bond of the α C-atom (C_α−H) without assistance from supports appears not to have been previously recognized; such properties seem plausible, however, in light of the known ability of Cu surfaces to activate C−H, C−O and O−H bonds[41] in oxygenates and to form adsorbed alkoxides that can act as basic moieties in condensation and esterification catalytic sequences. Intramolecular C-atoms (instead of H-atoms) are used to selectively remove oxygen from aldol species on all catalysts to form 3-pentanone, without requiring the presence of a support with basic properties. Decarbonylation was also observed by other authors[15] yielding n-pentane and CO from 2-methyl 2-pentenal using Pt and Pd catalyst but not on Cu surfaces. In section 3.2.4, we also show that the rates of formation of both propyl propionate and 3-pentanone are proportional to the number of Cu atoms exposed at surfaces of Cu clusters sufficiently large to preclude size effects on reactivity, thus confirming the monofunctional nature of both condensation and esterification pathways.

Cu metal is the prevalent phase during catalysis of propanol−propanal−H_2 mixtures at the conditions of our study. Rates of reduction during H_2 treatment showed that Cu oxide precursors convert to Cu metal at temperatures below 500 K. These samples were treated in H_2 at 553 K before catalytic measurements and used to convert reactant mixtures under reducing conditions that preserve Cu clusters in their metallic state based on thermodynamic considerations and the H_2/H_2O ratios prevalent during catalysis.

The results presented herein for the condensation of alkanols and alkanals demonstrate the ability of Cu metal clusters to form new C−C bonds and to remove O-atoms using C-atoms present within reactants (via decarbonylation or decarboxylation routes), thus preserving valuable H-atoms in the larger oxygenates formed. Concurrent water-gas sift reactions preclude the unequivocal identification of CO or CO_2, formed via decarbonylation or decarboxylation respectively, as the main coproduct of 3-pentanone synthesis.

3.2.3. Effects of Propanal, Propanol and H_2 Pressure on Condensation and Esterification Rates. The effects of reactant pressures on propanol−propanal−H_2 reaction rates and selectivities were examined at 503 K on 10% wt. Cu/SiO_2 samples (5.5% dispersion) diluted with SiO_2 to avoid any potential temperature or concentration gradients. Neither pellet diameter nor extent of dilution influenced measured rates or selectivities, thus ensuring that these rates reflect those of the chemical reactions without corruptions by transport artifacts. The only

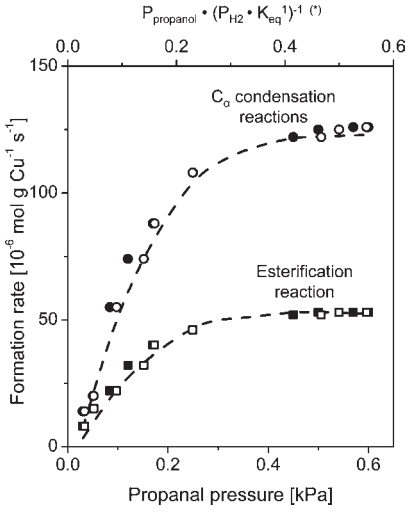

Figure 6. Formation rate for esterification (squares) and aldol condensation (circles) reactions from propanol−propanal−H_2 mixtures on 10% wt. Cu/SiO_2 (5.5% dispersion) as a function of propanal pressures (filled symbols) or $P_{propanol} \cdot (P_{H_2} \cdot K_{eq}^{1})^{-1}$ (open symbols); K_{eq}^{1}: equilibrium constant for propanal−propanol interconversion at 503 K.[28] Symbols: experimental data.

products detected at all conditions were propyl propionate (ester), 3-pentanone, 2-methyl-3-pentanone, 3-methylpentanal (aldol-type condensation products), CO, CO_2, and small amounts of 3-pentanol, 2-methyl-3-pentanol, 3-methylpentanol, propene, and propane; the combined selectivities to the latter two products were <6%.

Figure 6 shows esterification and condensation rates (extrapolated to zero residence time to avoid any conversion effects on rates or selectivities) as a function of the measured propanal pressures (bottom abscissa axis) or calculated from propanol and hydrogen pressures assuming thermodynamic equilibration [propanol pressure$\cdot$(H_2 pressure$\cdot K_{eq}^{1}$)$^{-1}$] (top abscissa axis) on 10% wt. Cu/SiO_2. These two curves are identical, consistent with the equilibrated nature of propanal−propanol interconversion. Propanol and propanal interconvert on Cu surfaces via adsorbed intermediates with an extent of dehydrogenation that depends on the H* coverage, set in turn via equilibrated H_2 dissociation steps. These steps are shown in Scheme 4 and involve the activation of O−H bond in propanol to form surface alkoxides ($CH_3CH_2CH_2O^*$), in a reaction that occurs on Cu(110) and Cu(111) surfaces at even subambient temperatures.[43−47] The resulting alkoxides readily dehydrogenate to alkanals at low temperatures (<370 K),[43−45] consistent with the fast propanol−propanal equilibration at all conditions in our study. Both condensation and esterification are thought to proceed by reactions of adsorbed alkanals with surface alkoxides ($C_3H_7O^*$) formed either by O−H dissociation in alkanols or partial hydrogenation of alkanals. The effects of H_2 and propanal (or propanol) pressures on condensation and esterification rates (shown below) suggest that propanal is the most abundant surface intermediate (MASI) and that it forms the intermediates required for C−O and C−C bond formation. Theoretical treatments support the basic character of adsorbed alkoxides and their tendency to preferentially activate acidic H-atoms at C_α-H bonds to form adsorbed enolates ($CH_3-CH^*-CH{=}O$).[48] The activation of the propanal by Cu metal surfaces, however, preferentially occurs at the carbonyl C−H bond to form a

Scheme 4. Propanol−Propanal Equilibration on Cu-based Catalysts

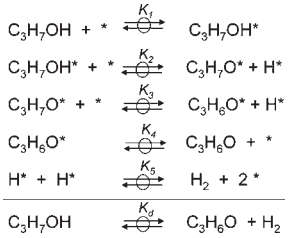

$CH_3CH_2C^*{=}O^*$ acyl intermediate with an activation energy of 97 kJ mol^{-1}, which is 40 kJ mol^{-1} higher than the barrier required for C_α−H bond activation by adsorbed propoxides. Scheme 5 shows the routes by which $CH_3-CH_2-C^*{=}O^*$ and $CH_3-CH^*-CH{=}O$ form C−O and C−C bonds in catalytic sequences that ultimately form esterification and condensation products.

Esterification is thought to proceed via nucleophilic attack by the basic oxygen in an adsorbed alkoxide ($CH_3-CH_2-CH_2-O^*$) or acyl ($CH_3-CH_2-C^*{=}O^*$) intermediate at the electrophilic C-atom in the carbonyl group of the adsorbed alkanal ($CH_3-CH_2-CH{=}O^*$). The resulting $C_6H_{13}O_2^*$ and $C_6H_{11}O_2^*$ intermediates dehydrogenate or hydrogenate, respectively, to form the corresponding ester, as in the accepted mechanism for base-catalyzed esterification.[35,39] Similar esterification paths have been reported for stoichiometric reactions between adsorbed alkoxides and alkanals on Au surfaces containing preadsorbed O* species and for catalytic reactions on nanoporous Au structures with residual Ag also in the presence of O_2.[46,47,49,50] These esterification reactions are examples of general nucleophilic substitutions involving reactions between coadsorbed electrophilic oxygenates and unsaturated hydrocarbons and carbonyls on metals, such as the addition of surface acetate, atomic oxygen or hydroxyl species to alkenes and alkanals, which form vinyl esters,[51,52] epoxides[53] and acids.[54] These bimolecular reactions between propanal and $CH_3-CH_2-CH_2-O^*$ or $CH_3-CH_2-C^*{=}O^*$ on Cu also resemble steps proposed for Tishchenko reactions of benzaldehyde on alkaline earth oxides,[55] in which vicinal alkanals adsorbed on basic (O^{2-}) and acidic cations are involved in rate-determining nucleophilic addition steps.

In contrast, C−C bonds form via nucleophilic addition of the bound α-carbon of the $CH_3-CH^*-CH{=}O$ enolate to the adsorbed carbonyl of the alkanal ($CH_3-CH_2-CH{=}O^*$) to form $HOCH_2-CH(R_1)-C(R_2)H-O^*$ alkoxides that dehydrogenate to the β-hydroxy aldol products (3-keto-, 2-methyl pentanol) and tautomerize to 3-hydroxy-2-methyl-pentanal. Neither aldol species are detected because of their slow desorption and fast decarbonylation or decarboxylation to form 3-pentanone or their dehydration-hydrogenation to form 2-methyl 3-pentanone and 2-methyl pentanal. Our results show that C=O or CO_2 removal reactions occur faster than dehydration-hydrogenation on Cu surfaces, leading to the preferential formation of 3-pentanone via monofunctional pathways on Cu clusters.

Plausible pathways for esterification and condensation reactions are shown in Schemes 6 and 7. The similar effects of reactant concentrations on esterification and condensation rates (Figures 6 and 7) suggest that the pathways involve kinetically relevant steps with intermediates of similar extents of dehydrogenation and that the same kinetic rate equation, albeit with

Scheme 5. Possible Mechanism for Esterification and Condensation Reactions from Propanal−Propanol Mixtures on Cu Catalysts

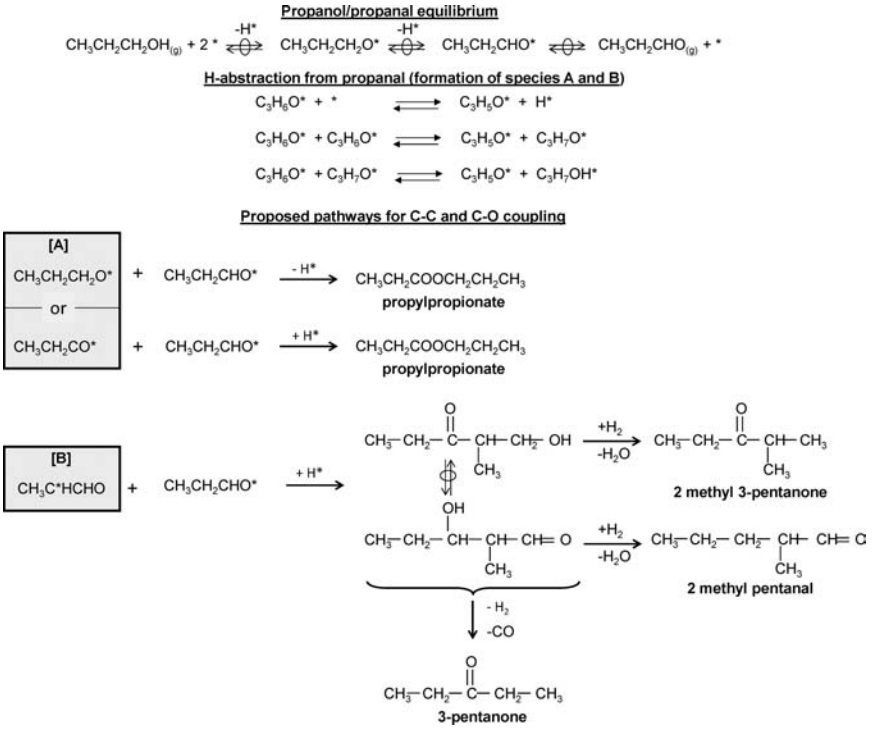

Scheme 6. Mechanism Proposed for 3-Pentanone Formation from Propanol−Propanal Intermediate on Cu Catalysts

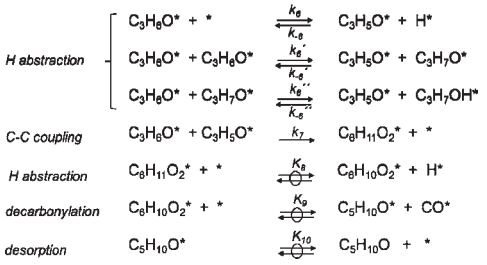

Scheme 7. Mechanisms Proposed for Propyl Propionate Formation from Propanol−Propanal Intermediate on Cu Catalysts

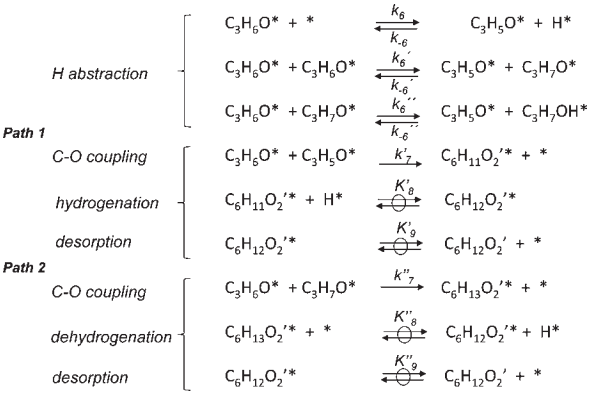

different kinetic constants, accurately describes the rates of both reactions.

The formation of 3-pentanone (Scheme 6) and propyl propionate (Path 1 Scheme 7) involves the activation of the C_α-H bond in adsorbed propanal by a vacant site (*) (Step 6, Case i), by another adsorbed propanal (Step 6′, Case ii), or by vicinal $C_3H_7O^*$ species (Step 6″, Case iii) (Schemes 6 and 7) to form $C_3H_5O^*$ intermediates, which subsequently react with adsorbed propanal in kinetically relevant C−C and C−O bond formation steps. More specifically, the rate equation for the formation of propyl propionate, which involves the reaction of adsorbed propanal with a surface propoxide (Path 2, Scheme 7; Case iv), is equivalent in functional form to the rate equation for condensation, which reflects hydrogen abstraction from adsorbed propanal by a surface propoxide, because both reactions and rate equations involve reactions between the same two intermediates ($CH_3CH_2CH_2O^* + CH_3CH_2CH{=}O^*$), albeit to form different products, in their respective kinetically relevant steps. $C_3H_5O^*$ is used here to denote $CH_3{-}CH_2{-}CH_2{-}C^*{=}O^*$ or $CH_3{-}CH_2{-}CH^*{-}CHO$ intermediates, because rate data and their mechanistic analysis cannot discern the location of the C−H bond activation event and of the subsequent attachment of its products to the surface.

Each of the four possible cases discussed above gives a different rate equation, the functional form of which must describe both esterification and condensation rates, in light of their similar measured kinetic behavior. The rate equations for Cases i−iii, involving propanal reactions with $C_3H_5O^*$, each have two limiting forms, corresponding to the extreme cases of quasi-equilibrated or irreversible H-abstraction steps. The irreversible condensation and esterification reactions in

dx.doi.org/10.1021/ja207551f |J. Am. Chem. Soc. 2011, 133, 20384–20398

Case iv are different from those in Case iii, but the resulting kinetic expressions are the same, because the kinetically relevant steps for the C−O and C−C reactions in Cases iii and iv involve $C_3H_6O^*$ reactions with $C_3H_7O^*$, as discussed above. The kinetic and adsorption constants for Case iv, however, differ from those in Case iii, because of the different products that form in these two cases (Table 4).

The seven resulting rate equations (derived in Section S2, Supporting Information) are:

(i.1.) Quasi-equilibrated Step 6

$$r = A_1 \cdot \frac{[C_3H_6O]^2 \cdot [H_2]^{-0.5}}{(1 + B \cdot [C_3H_6O] + C \cdot [C_3H_6O] \cdot [H_2]^{0.5} + D \cdot [C_3H_6O] \cdot [H_2] + E \cdot [H_2]^{0.5})^2} \quad (1)$$

(i.2) Irreversible Step 6

$$r = A_2 \cdot \frac{[C_3H_6O]}{(1 + B \cdot [C_3H_6O] + C \cdot [C_3H_6O] \cdot [H_2]^{0.5} + D \cdot [C_3H_6O] \cdot [H_2] + E \cdot [H_2]^{0.5})^2} \quad (2)$$

(ii.1) Quasi-equilibrated Step 6′

$$r = A_3 \cdot \frac{[C_3H_6O]^2 \cdot [H_2]^{-0.5}}{(1 + B \cdot [C_3H_6O] + C \cdot [C_3H_6O] \cdot [H_2]^{0.5} + D \cdot [C_3H_6O] \cdot [H_2] + E \cdot [H_2]^{0.5})^2} \quad (3)$$

(ii.2) Irreversible Step 6′

$$r = A_4 \cdot \frac{[C_3H_6O]^2}{(1 + B \cdot [C_3H_6O] + C \cdot [C_3H_6O] \cdot [H_2]^{0.5} + D \cdot [C_3H_6O] \cdot [H_2] + E \cdot [H_2]^{0.5})^2} \quad (4)$$

(iii.1) Quasi-equilibrated Step 6″

$$r = A_5 \cdot \frac{[C_3H_6O]^2 \cdot [H_2]^{-0.5}}{(1 + B \cdot [C_3H_6O] + C \cdot [C_3H_6O] \cdot [H_2]^{0.5} + D \cdot [C_3H_6O] \cdot [H_2] + E \cdot [H_2]^{0.5})^2} \quad (5)$$

(iii.2) Irreversible Step 6″

$$r = A_6 \cdot \frac{[C_3H_6O]^2 \cdot [H_2]^{0.5}}{(1 + B \cdot [C_3H_6O] + C \cdot [C_3H_6O] \cdot [H_2]^{0.5} + D \cdot [C_3H_6H_6O] \cdot [H_2] + E \cdot [H_2]^{0.5})^2} \quad (6)$$

(iv) Irreversible Step 7′

$$r = A_7 \cdot \frac{[C_3H_6O]^2 \cdot [H_2]^{0.5}}{(1 + B \cdot [C_3H_6O] + C \cdot [C_3H_6O] \cdot [H_2]^{0.5} + D \cdot [C_3H_6O] \cdot [H_2] + E \cdot [H_2]^{0.5})^2} \quad (7)$$

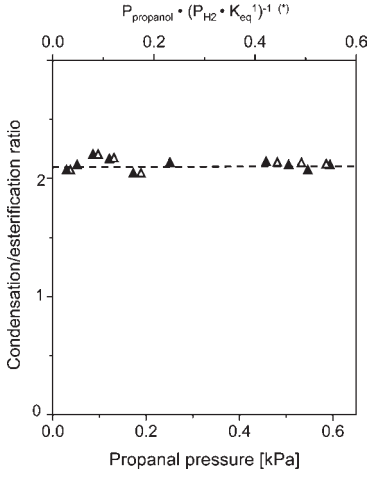

Figure 7. Condensation/esterification ratio for propanol−propanal−H_2 mixtures on 10% wt. Cu/SiO_2 (5.5% dispersion) as a function of propanal pressures (filled symbols) or $P_{propanol} \cdot (P_{H_2} \cdot K_{eq}^{-1})^{-1}$ (open symbols); K_{eq}^{-1}: equilibrium constant for propanal−propanol interconversion at 503 K.[28]

The parameters, A_i (i = 1−7 for 3-pentanone formation) and A'_i (i = 1−7 for propyl propionate formation) are defined in Table 4 and contain kinetic and adsorption constants for elementary steps. The terms B, C, D and E in each of these expressions refer to the adsorption and reaction equilibrium constants that determine the surface coverages of propanal ($1/K_4$), propoxide ($K_1K_2K_5^{0.5}/K_d$), and hydrogen atoms ($1/K_5^{0.5}$) and reflect the relative coverages of species at surfaces that are common to both esterification and condensation reactions. The regressed values for B and C are presented in Table 5 for Cases i.2, ii.2 and iii.3).

An initial regression analysis of these equations showed that the denominator term for all cases does not contain detectable contributions from the terms for $C_3H_7OH^*$ ($D[C_3H_6O][H_2]$) and H^* ($E[H_2]^{0.5}$). Therefore, eqs 1−7 were ultimately regressed without these terms for both condensation and esterification rate data. All irreversible Cases (i, ii, iii, and iv) provided acceptable fits to the rate data (Supporting Information) suggesting that we cannot distinguish based on these data whether $C_3H_6O^*$ is activated by *, $C_3H_6O^*$, $C_3H_5O^*$ or $C_3H_7O^*$ surface intermediates. The regressed kinetic parameters for these four

dx.doi.org/10.1021/ja207551f | J. Am. Chem. Soc. 2011, 133, 20384–20398

Table 4. Definitions of the Kinetic Parameters Involved in eqs 1−7 for Propanol−Propanal Condensation Reactions

kinetic parameter	reactions[a]
3-Pentanone formation	
A_1	$\frac{k_7 \cdot K_S^{0.5} \cdot K_6}{K_4^2}$
A_2	$\frac{k_6}{K_4}$
A_3	$\frac{k_7 \cdot K_3 K_S^{0.5} K_6'}{K_4}$
A_4	$\frac{k_6'}{K_4}$
A_5	$\frac{k_7 \cdot K_2 K_S^{0.5} K_6''}{K_4^2}$
A_6	$\frac{k_6''}{K_3 K_4 K_S^{0.5}}$
A_7	$\frac{k_7'}{K_3 K_4^2 K_S^{0.5}}$
Propyl propionate formation	
A'_1	$\frac{k_{7'} \cdot K_S^{0.5} \cdot K_6}{K_4^2}$
A'_2	$\frac{k_6}{K_4}$
A'_3	$\frac{k_{7'} \cdot K_3 \cdot K_S^{0.5} \cdot K_6'}{K_4^2}$
A'_4	$\frac{k_6'}{K_4}$
A'_5	$\frac{k_{7'} \cdot K_2 \cdot K_S^{0.5} \cdot K_6''}{K_4^2}$
A'_6	$\frac{k_6''}{K_3 K_4 K_S^{0.5}}$
A'_7	$\frac{k_{7'}'}{K_3 K_4 K_S^{0.5}}$
3-Pentanone and propyl propionate formation	
B	$\frac{1}{K_4}$
C	$\frac{K_1 \cdot K_2 \cdot K_S^{0.5}}{K_d}$
D	$\frac{K_1}{K_d}$
E	$\frac{1}{K_S^{0.5}}$

[a] k'_7 is the rate constant for the irreversible reaction between $C_3H_7O^*$ and $C_3H_6O^*$ species to form the new C−C bond via aldol type reaction (k'_7' is the rate constant for the irreversible reaction between $C_3H_7O^*$ and $C_3H_6O^*$ species to form propyl propionate).

cases (i.2, ii.2, iii.2, and iv) are presented in Table 5 and their plausible contributions to measured rates are discussed below in the context of analogies with known esterification and condensation mechanisms on bases.

Table 5. Estimated Parameters of Kinetic Equations for Propyl Propionate and 3-Pentanone Formation According to eqs 2, 4 and 6−7[a]

estimated parameter	numerical value
Case (i.2)	
A_2 [10^{-6} mol·(g Cu·s)$^{-1}$·kPa^{-2}][b]	814
A'_2 [10^{-6} mol·(g Cu·s)$^{-1}$·kPa^{-2}][c]	388
B (kPa^{-1})	1.7
C (kPa$^{-1.5}$)	0.002
Case (ii.2)	
A_4 [10^{-6} mol·(g Cu·s)$^{-1}$·kPa^{-2}][b]	59000
A'_4 [10^{-6} mol·(g Cu·s)$^{-1}$·kPa^{-2}][c]	28000
B (kPa^{-1})	19.5
C (kPa$^{-1.5}$)	0.20
Case (iii.2 or iv.)	
A_6 [10^{-6} mol·(g Cu·s)$^{-1}$·kPa$^{-2.5}$][b]	1300
A'_6 [10^{-6} mol·(g Cu·s)$^{-1}$·kPa$^{-2.5}$][c]	622
B (kPa^{-1})	3.3
C (kPa$^{-1.5}$)	0.008

[a] 503 K, 10% wt. Cu/SiO_2, 5.5% dispersion. [b] For 3-pentanone formation. [c] For propyl propionate formation.

The activation of propanal by vacant sites (*; case i.2) is likely to proceed via homolytic metal atom insertion into the C−H bond, making the carbonyl C−H bond more reactive than the C−H bond at the α-position, in view of its smaller homolytic dissociation energy (by 29 kJ/mol for propanal).[48] The preferential abstraction of the H-atom at the α-position is evident from the preferential formation of 3-pentanone via classical aldol condensation routes, making activation of the carbonyl C−H bond implausible to account for condensation products and by inference, because of their similar rate equations, also for esterification reactions.

Case ii.2 implies that condensation and esterification are controlled by intermolecular H-transfer between vicinal propanals, a step that seems highly unlikely as it would require the activation and transfer of hydrogen between two weakly bound stable molecules in a rather endothermic step. We are not aware of any reported intramolecular hydrogen transfer reactions between stable unsaturated species on metal surfaces.

The H-abstraction step in Case iii.2 seems more plausible than those in Case i.2 or ii.2 because it involves reactions of the acidic C_α−H bond with vicinal basic propoxides, in a step analogous to the reactions of basic O-atoms in bases in aldol condensations (as discussed in section 3.2.1). Case iii would also require H-abstraction from the carbonyl group of adsorbed propanal by vicinal propoxide species for both condensation and esterification reactions; theoretical estimates show that the energy required for H-abstraction from the carbonyl position of propanal by OH^-(g) in the gas phase is ~60 kJ/mol greater than for reactions at the acidic α-position.[48] In addition, the unsaturated acyl intermediate that results binds strongly to metal surfaces (>220 kJ/mol)[56] thus making it much less reactive in the C−C bond formation reactions that would require the ultimate cleavage of these strong metal-acyl bonds.

The reaction of adsorbed propanal with a surface propoxide (Case iv) seems the most plausible route among the four routes consistent with the rate data. The resulting rate equation accurately describes condensation and esterification rate data

and is consistent with the chemical events that mediate base-catalyzed condensation and esterification reactions. Condensation proceeds via H-abstraction of the acidic hydrogen at the α-position in propanal by an adsorbed propoxide, acting as the base. This step forms $CH_3-C^*H-CH_2=O$ surface enolates that react with adsorbed propanal via nucleophilic attack to form 3-hydroxy-2methyl pentanal and 3-keto-2methyl pentanol aldol products depicted in the C_α-paths in Scheme 3. Adsorbed propoxides act as the base to catalyze C_α enolate formation, consistent with the predominance of C_α over C_β paths involving weakly acidic hydrogen at the C_β position, which suggests, in turn, the involvement of a base in the H-abstraction step. In this mechanistic case, esterification involves direct nucleophilic attack of adsorbed propoxide intermediates on coadsorbed propanal, to form $C_6H_{13}O_2^*$ species that dehydrogenate to give propyl propionate. These steps represent the accepted mechanism for base-catalyzed esterifications.[35,40]

These mechanistic interpretations of esterification and condensation rate data lead us to conclude that C−C and C−O bond formation paths involve kinetically relevant reactions of $CH_3CH_2CH_2O^*$ with $CH_3CH_2CH=O^*$ to form either the $C_3H_5O^*$ enolate, which reacts with another propanal to give the aldol, or the $C_6H_{13}O_2^*$ intermediate, which dehydrogenates to propyl propionate. In these pathways, weakly adsorbed alkoxides on Cu serve as the base that mediates the H-abstraction to form the adsorbed enolate in the condensation path and the nucleophile that directly reacts with propanal in the esterification path.

The rate expression for the condensation reaction in Case iv is given in eq 8, in which the relevant kinetic constant is k_6''. The esterification reaction for Case iv is identical with the sole exception that the intrinsic rate constant is k_7' instead (eq 9). The regressed parameters for condensation and esterification are given in eqs 10 and 11, respectively.

$$v = \frac{k_6''}{K_3 \cdot K_4^2 \cdot K_5^{0.5}} \cdot \frac{[C_3H_6O]^2 \cdot [H_2]^{0.5}}{\left(1 + \frac{1}{K_4} \cdot [C_3H_6O] + \frac{K_1 \cdot K_2 \cdot K_5}{K_d} \cdot [C_3H_6O] \cdot [H_2]^{0.5}\right)^2} \tag{8}$$

$$v = \frac{k_7'}{K_3 \cdot K_4^2 \cdot K_5^{0.5}} \cdot \frac{[C_3H_6O]^2 \cdot [H_2]^{0.5}}{\left(1 + \frac{1}{K_4} \cdot [C_3H_6O] + \frac{K_1 \cdot K_2 \cdot K_5}{K_d} \cdot [C_3H_6O] \cdot [H_2]^{0.5}\right)^2} \tag{9}$$

$$v = 1.3 \times 10^{-3} \text{mol} \cdot (\text{gCu} \cdot \text{s})^{-1} \text{kPa}^{-2.5} \cdot \frac{[C_3H_6O]^2 \cdot [H_2]^{0.5}}{(1 + 3.3 \cdot [C_3H_6O] + 0.008 \cdot [C_3H_6O] \cdot [H_2]^{0.5})^2} \tag{10}$$

$$v = 0.62 \times 10^{-3} \text{mol} \cdot (\text{gCu} \cdot \text{s})^{-1} \text{kPa}^{-2.5} \cdot \frac{[C_3H_6O]^2 \cdot [H_2]^{0.5}}{(1 + 3.3 \cdot [C_3H_6O] + 0.008 \cdot [C_3H_6O] \cdot [H_2]^{0.5})^2} \tag{11}$$

The second term in the denominator reflects $C_3H_6O^*$ coverage. Its value ranges from 0.3 to 1.5 over the range of pressures used to obtain these rate data; the comparable value for $C_3H_7O^*$ (the last denominator term) is much smaller (<0.05) indicating that propanal intermediates are the most abundant surface species during steady-state catalysis.

3.2.4. Effects of Cu Cluster Size on Condensation and Esterification Turnover Rates. In this last section, we consider the effects of Cu cluster size (and dispersion) on condensation and esterification turnover rates in the context of the mechanistic proposals described above, taken together with the expected effects of surface coordination on the binding energy of reactive intermediates and on the stability of plausible transition states for the kinetically relevant steps. These effects were specifically examined using propanol−propanal−H_2 reactions (at conditions leading to their equilibrated interconversion) on 5−20% wt. Cu/SiO_2 catalysts with a broad range of dispersion (2−17%) and mean cluster diameter (5−55 nm).

The results are shown in Table 6 as pool conversion turnover rates (as mol [mol of surface Cu-s]$^{-1}$, surface Cu determined by N_2O titration) for these catalysts at three H_2 pressures as a function of Cu dispersion. The effects of Cu dispersion and H_2 pressure (or propanal pressure) on condensation and esterification turnover rates are also shown in Figure 8a and b. Cu dispersions between 2 and 5.5% did not influence turnover rates, which then decreased at higher dispersions at all H_2 pressures; these different H_2 pressures set equilibrium propanal−propanol ratios and the extent of dehydrogenation of adsorbed intermediates, but not the identity or the rate constants for kinetically relevant steps.

These trends indicate that low-index planes, which prevail on large clusters, exhibit higher reactivity for both condensation and esterification reactions. Coordinatively unsaturated surface Cu atoms at corners and edges of small clusters are expected to bind all adsorbed species more strongly, based on simple bond-order bond-energy considerations; such strong binding sites appear to stabilize adsorbed precursors more strongly than their transition states, thus increasing activation barriers for the kinetically relevant elementary steps. Such higher barriers can be compensated, at least in part, by a concomitant increase in the coverage of these of intermediates, as long as they are present at coverages below saturation. These effects are evident from the form of the rate equations (eqs 8 and 9) for both reactions and from the predominant contributions from their first and second denominator terms at the conditions used to measured the rate data in Figures 8a and b, which corresponds to fractional $C_3H_6O^*$ coverages from 0.25 (at 80 kPa H_2) to ~0.6 (at 20 kPa H_2) for 10 wt % Cu/SiO_2. Therefore, the rate data in Figure 8 reflect the combination of kinetic constants in the numerator for condensation ($k_6''/K_2K_4^2K_5^{0.5}$) and esterification ($k_7'/K_2K_4^2K_5^{0.5}$)

Table 6. Effect of Cu Dispersion and Average Crystallite Diameter on Propanol/Propanal Pool Turnover Rates in the Presence of H_2[a]

	treatment				pool turnover rates (s^{-1})[c] H_2 pressure (kPa)		
Cu content (% wt.)	Dry air	H_2	Cu dispersion (%)	Cu drystallite diameter[b] (nm)	20	50	80
10	773 K, 5 h	553 K, 2 h	9.0	11	0.120	0.082	0.062
10	823 K, 5 h	553 K, 2 h	7.0	14	0.167	0.103	0.080
10	873 K, 2 h	553 K, 2 h	5.5	20	0.200	0.137	0.096
10	923 K, 2 h	553 K, 2 h	4.0	26	0.203	0.139	0.095
10[d]	548 K, 1 h	553 K, 2 h	12.5	8	0.039	0.034	0.022
20	773 K, 5 h	553 K, 2 h	2.0	55	0.205	0.150	0.101
5	923 K, 2 h	553 K, 2 h	5.6	20	0.199	0.137	0.095
5 [d]	548 K, 1 h	553 K, 2 h	17.0	5	0.025	0.025	0.017

[a] Cu/SiO_2, 503 K, 0.64 kPa propanol, balance He. [b] Estimated from Cu fractional dispersion assuming hemispherical clusters. [c] Units of (mol of propanol)/(mol of surface Cu-s). [d] Using triethanolamine (TEA) as the impregnation aid (molar ratio of Cu/TEA = 1).

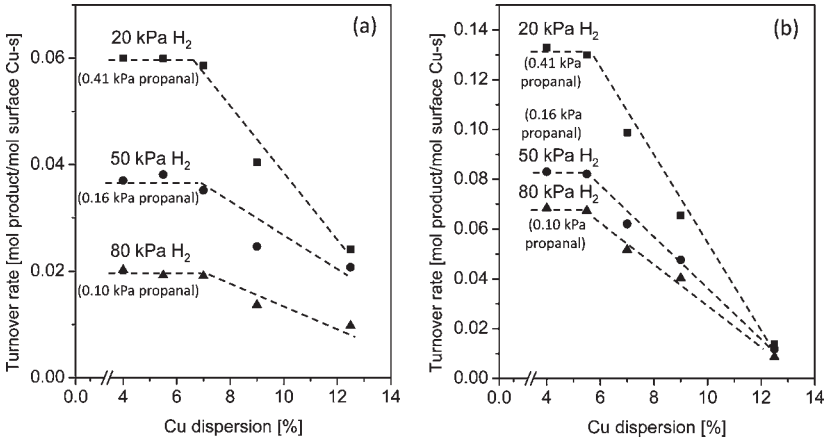

Figure 8. Site-time yield as a function of Cu dispersion for propanol−propanal−H_2 reactions on 10% wt. Cu/SiO_2 samples. (a) Esterification reaction; (b) condensation reactions (503 K, 0.64 kPa propanol, balance He).

divided by the $(1 + B\ [C_3H_6O])^2$ denominator terms that contain the adsorption equilibrium constant for propanal ($B = 1/K_4$). The effects of dispersion therefore balance the effects of surface coordination on the reactivity of adsorbed species and on their binding energy and coverage in the mathematical form dictated by eqs 8−11.

We address next how kinetic and thermodynamic parameters in these rate equations sense the coordination of Cu surface atoms. Rate constants (k_6'', k_7') reflect barriers for reactions between propoxides and propanal species involving hydrogen abstraction (for condensation) and nucleophlic attack (for esterification). Stronger binding of propoxides by coordinatively unsaturated sites would decrease their basicity and reactivity, as well as the receptivity of the vicinal alkanal for H-abstraction or nucleophilic attack, thus increasing the respective activation barriers. In both reactions, the required cleavage of the metal−propoxide causes reactants to be preferentially stabilized over transition states by a decrease in surface atom coordination. Indeed, barriers for bond-making and H-transfer steps involving strongly adsorbed species increase proportionately with adsorption energies,[57] as shown by Brønsted-Evans-Polanyi relations for the early transition states that typically mediate these processes.[57,58] These concepts lead us to conclude that kinetic constants (k_6'', k_7') for the relevant condensation and esterification steps would decrease as the average surface coordination decreases with increasing Cu dispersion.

These rate constants appear in the numerator divided by a $(K_2K_4^2K_5^{0.5})$ term and by a $[1+ (C_3H_6O)/K_4)]^2$ denominator term in which K_2, $1/K_4$, and $1/K_5$ (the reciprocals reflect the desorption direction in which steps 4 and 5 are written in Scheme 4) increase as H* and C_3H_6O* becomes more strongly bound with decreasing surface coordination. Their effects of coordination on their combined contributions are likely to be much weaker than for the kinetic parameters (k_6'', k_7') as a result of the partial cancelation of K_4 terms in the numerator and denominator and of the opposite effects of coordination on K_2 and K_5, leading to overall condensation and esterification rates that decrease as the coordination of exposed metal atoms decreases with increasing dispersion (Figures 8a and 8b)

In our mechanistic interpretation of these rate data and cluster size effects, alkoxides act as bases, rendering Cu metal surfaces active in condensation and esterification reactions commonly catalyze by basic catalysts. These organic bases bind weakly as anionic species on group VIII metals with filled d-bands and can act as bases, in a manner analogous to O* species chemisorbed on such metals, in H-abstraction or nucleophilic attack. Indeed, Au-based catalysts catalyze the condensation, but not the esterification, of equilibrated alkanol-alkanal reactants, apparently

also via basic alkoxides that mediate the kinetically relevant H-abstraction steps. Esterification of alkanols have also been detected on Au single crystals and nanoporous Au (with trace Ag residues from their synthesis) when oxygen is present, either as stoichiometric O*[46,47,49] or as O_2 coreactants,[50] respectively. In these cases, weakly bound O* abstract H-atoms from alkanols to form reactive alkoxides, which are involved in nucleophilic attack on coadsorbed alkanals to form esters. Glycerol and alkanols oxidations using stoichiometric addition of base (OH-) to bulk Au catalysts[54] involve OH- reactions that abstract H-atoms from reactants for form alkanals, which then undergo nucleophilic attack, in this case by OH- to form acids, instead of alkoxides to form esters or aldols, because of the prevalence of OH- species at the pH used in these reactions.

4. CONCLUSIONS

The selective removal of oxygen from prototypical alkanediol, alkanol, and alkanal biomass derived molecules was catalyzed by dispersed Cu clusters using minimal external H_2 with concomitant formation of new C−C and C−O bonds. The oxygen atoms were removed via two different types of reactions involving intramolecular utilization of C-atoms to eliminate O-atoms by decarbonylation/decarboxylation and hydrogenolysis or hydrogenation via H-atoms extracted by CO from H_2O as a result of the water gas shift reaction as opposed to the alternative on-purpose generation and use of H_2. More specifically, we show that equilibrium mixtures of propanol and propanal rapidly form from 1,3-propanediol using *in situ* generated H_2 via the water gas shift reaction, external H_2 or even without coreactants using Cu-based catalyst.

Surprisingly, copper alone was found to directly catalyze chain lengthening alkanal and alkanol condensation and esterification reactions without requiring the presence of a basic support. In contrast with condensation reactions carried out over acid or base catalysts which result in the formation of β-hydroxy carbonyls that subsequently undergo dehydration to form C_{2n} oxygenates (i.e., 2-methyl pentanal and 2-methyl 3-pentanone), the main product over supported Cu was 3-pentanone produced by further decarbonylation/decarboxylation of aldol intermediate species thus preserving valuable H-atoms within the products and proving that internal C-atoms can be successfully used to remove oxygen from these molecules. These same monofunctional Cu clusters also catalyzed C−O bond making reactions forming propyl propionate ester from propanal−propanol−H_2 mixtures at the reaction conditions used in this work. The formation rates of the ester and the aldol intermediate were directly proportional to the number of exposed Cu atoms, thus indicating that monofunctional Cu catalyzes these reactions.

Kinetic data showed that equilibrium mixtures of propanol, propanal and hydrogen form over supported Cu and react via C−C and C−O bond formation paths involving the same kinetically relevant steps between adsorbed propanal and basic surface propoxide. The propoxide can catalyze the abstraction of the acidic C_α−H from a vicinal propanal to form a surface enolate that can subsequently react with a neighboring propanal to form the aldol intermediates which can then decabonylate/decarboxylate to form the 3-pentanone. Alternatively, the basic propoxide intermediate can also react directly with an adsorbed propanal via nucleophilic attack at the electrophilic carbonyl of the adsorbed propanal to form the $C_6H_{13}O_2$* intermediate that dehydrogenates to the propyl propionate ester. In both condensation and esterification pathways, Cu and hydrogen catalyze the in situ formation of weakly adsorbed propoxide that acts as a base to catalyze H-abstraction from propanal to form the adsorbed enolates in the condensation path and nucleophilic attack on a vicinal propanal in the esterification pathway.

Both condensation and esterification reactions show similar changes in their rates as a function of Cu cluster size and hydrogen pressure. The reported turnover frequencies for both reactions were insensitive to decreasing Cu dispersions to greater than 7.5% due to the predominance of the fraction of coordinatively saturated sites on the larger Cu clusters. The turnover rates however decreased linearly with increasing Cu dispersions above 7.5% as a result of the increasing fraction of coordinatively unsaturated sites on the smaller Cu clusters which bind the propanal and propoxide intermediates more strongly and thus increase the barriers of the kinetically relevant steps that dominate the measured esterification and condensation rates.

■ ASSOCIATED CONTENT

Supporting Information. Section S1 in Supporting Information includes structural characterization data for the Cu/ZnO/Al_2O_3 catalyst, specifically the X-ray diffractograms of the hydrotalcite-like structure formed via coprecipitation of Cu, Zn and Al nitrates and of this sample after treatment in He for 8 h at 673 K. Section S2 describes the derivation of the rate equations for condensation and esterification reactions based on the identity and kinetic relevance of the elementary steps proposed in the main text using standard methods based on the pseudo-steady-state approximation. It also shows comparisons between measured rates and those predicted from these various mechanistic interpretations in the form of parity plots for 3-pentanone and propyl propionate, the respective products of condensation and esterification reactions. This material is available free of charge via the Internet at http://pubs.acs.org.

■ AUTHOR INFORMATION

Corresponding Author
iglesia@berkeley.edu

■ ACKNOWLEDGMENT

We acknowledge the support from BP as part of the Methane Conversion Cooperative Research Program at the University of California at Berkeley and the University of Virginia. We thank Prof. De Chen (Norwegian University of Science and Technology), Dr. Dante Simonetti (UC-Berkeley), Mr. Konstantinos Goulas (UC-Berkeley), Professor John Bercaw (California Institute of Technology), Professor Robert H. Grubbs (California Institute of Technology) and Professor Jay Labinger (California Institute of Technology) for valuable technical insights and comments.

■ REFERENCES

(1) Huber, G. W.; Iborra, S.; Corma, A. *Chem. Rev.* **2006**, *106*, 4044.
(2) Román-Leshkov, Y; Barrett, C. J.; Liu, Z. Y.; Dumesic, J. A. *Nature* **2007**, *447*, 982.
(3) Chheda, J. N.; Huber, G. W.; Dumesic, J. A. *Angew. Chem., Int. Ed.* **2007**, *46*, 7164.
(4) Newsome, D. S. *Catal. Rev. Sci. Eng.* **1980**, 21.
(5) Escaffre, P.; Thorez, A.; Kalck, P. *J. Mol. Catal.* **1985**, *33*, 87.

(6) Owen, H.; Rosinski, E. J.; Venuto, P. B. US Patent 3,974,062, 1976.
(7) Davda, R. R.; Shabaker, J. W.; Huber, G. W.; Cortright, R. D.; Dumesic, J. A. *Appl. Catal. B: Env.* **2005**, *56*, 171.
(8) Cortright, R. D.; Madison, W. I.; Blommel, P. G. US 2008/0216391 A1.
(9) Hassan, A.; Land, S.; Bagherzadeh, E.; Anthony, R. G.; Borsinger, G.; Hassan, A. US 2009/0001316 A1.
(10) Campbell, C. T.; Daube, K. A. *J. Catal.* **1987**, *104*, 109.
(11) Petrini, G.; Garbassi, F. *J. Catal.* **1984**, *90*, 113.
(12) Kraus, M. In *Handbook of Heterogeneous Catalysis*, Vol. 4; Ertl, G., Knözinger, H., Weitkamp, J., Eds.; Wiley−VCH: Weinheim, 1997.
(13) Xu, M.; Gines, M. J. L.; Hilmen, A. M.; Stephens, B. L.; Iglesia, E. *J. Catal.* **1997**, *171*, 130.
(14) Han, Y.; Shen, J.; Chen, Y. *Appl. Catal., A* **2001**, *205*, 79.
(15) Pham, T. T.; Lobban, L. L.; Resasco, D. E.; Mallinson, R. G. *J. Catal.* **2009**, *266*, 9.
(16) Chheda, J. N.; Dumesic, J. A. *Catal. Today* **2007**, *123*, 59.
(17) West, R. M.; Liu, Z. Y.; Peter, M.; Gartner, C. A.; Dumesic, J. A. *J. Mol. Catal. A: Chem.* **2008**, *296*, 18.
(18) West, R. M.; Liu, Z. Y.; Peter, M.; Dumesic, J. A. *Chemsuschem* **2008**, *1*, 417.
(19) Wade, L. G. *Organic Chemistry*, 6th ed.; Prentice Hall: Upper Saddle River, NJ, 2005.
(20) Hamilton, C. A.; Jackson, S. D.; Kelly, G. J. *Appl. Catal. A:Gen.* **2004**, *263*, 63.
(21) Palomares, A. E.; Eder-Mirth, G.; Rep, M.; Lercher, J. A. *J. Catal.* **1998**, *180*, 56.
(22) Engelhardt F., Schritt W. US Patent 3,558,716, 1965.
(23) Veibel, S.; Nielsen, J. I. *Tetrahedron* **1967**, *23* (4), 1723–1733.
(24) Takeshita, K.; Nakamura, S.; Kawamoto, K. *Bull. Chem. Soc. Jpn.* **1978**, *51*, 2622.
(25) Kim, D. K.; Iglesia, E. *J. Phys. Chem. C* **2008**, *112*, 44.
(26) Chinchen, G. C.; Hay, C. M.; Vandervell, H. D.; Waugh, K. C. *J. Catal.* **1987**, *103*, 79.
(27) Mastalir, A.; Frank, B.; Szizybalski, A.; Soerijanto, H.; Deshpande, A.; Niederberger, M.; Schomäcker, R.; Schlögl, R.; Ressler, T. *J. Catal.* **2005**, *230*, 464.
(28) Stull, D. R., Westrum, E. F., Sinke, G. C. *The Chemical Thermodynamics of Organics Compounds*; John Wiley & Sons, Inc.: New York, 1969.
(29) Sato, S.; Akiyama, M.; Takahashi, R.; Hara, T.; Inui, K.; Yokota, M. *Appl. Catal. A: Gen* **2008**, *347*, 186.
(30) Gines, M. J. L.; Iglesia, E. *J. Catal.* **1998**, *176*, 155.
(31) Elliot, D. J.; Pennella, F. *J. Catal.* **1989**, *119*, 359.
(32) Gines, M. J. L.; Amadeo, N.; Laborde, M.; Apesteguia, C. R. *Appl. Catal. A: Gen.* **1995**, *131*, 283.
(33) Bowker, M.; Madix, R. J. *Surf. Sci.* **1982**, *116*, 549.
(34) Dandekar, A.; Baker, R. T. K.; Vannice, M. A. *J. Catal.* **1999**, *184*, 421.
(35) Hattori, H. *Chem. Rev.* **1995**, *95* (3), 537.
(36) Sharma, S. K.; Parikh, P. A.; Jasra, R. V. *J. Mol. Catal. A: Chem.* **2007**, *278*, 135.
(37) Ueda, W.; Kuwabara, T.; Ohshida, T.; Morizawa, Y. *J. Chem. Soc., Chem. Comm.* **1990**, 1558.
(38) Komarewsky, V. I.; Coley, J. R. *J. Am. Chem. Soc.* **1942**, *63* (700), 3269.
(39) Tishchenko, V. *J. Russ. Phys. Chem. Soc.* **1906**, *38*, 355. 482. 540. 547.
(40) Cannizzaro, S. *Ueber den der Benzoësäure entsprechenden Alkohol* **1853**, *88*, 129–130.
(41) Batyrev, E. D.; van den Heuvel, J. C.; Beckers, J.; Jansen, W. P. A.; Castricum, H. L. *J. Catal.* **2005**, *229*, 136.
(42) Bowker, M.; Madix, R. J. *Surf. Sci.* **1980**, *95* (1), 190.
(43) Carley, A. F.; Owens, A. W.; Rajumon, M. K.; Roberts, M. W.; Jackson, S. D. *Catal. Lett.* **1996**, *37* (1−2), 79.
(44) Polmann, S.; Bayer, A.; Ammon, C.; Steinruck, H. P. *Z. Phys. Chem.−Int. J. Res. Phys. Chem. Chem. Phys.* **2004**, *218* (8), 957.
(45) Ammon, C.; Bayer, A.; Held, G.; Richter, B.; Schmidt, T.; Steinruck, H. P. *Surf. Sci.* **2002**, *507*, 845.
(46) Liu, X. Y.; Xu, B. J.; Haubrich, J.; Madix, R. J.; Friend, C. M. *J. Am. Chem. Soc.* **2009**, *131* (16), 5757.
(47) Xu, B. J.; Liu, X. Y.; Haubrich, J.; Friend, C. M. *Nat. Chem.* **2009**, *2*, 61.
(48) Tao, Z.; Neurock, M. unpublished.
(49) Xu, B. J.; Liu, X. Y.; Haubrich, J.; Madix, R. J.; Friend, C. M. *Angew. Chem., Int Ed.* **2009**, *48* (23), 4206.
(50) Wittstock, A.; Zielasek, V.; Biener, J.; Friend, C. M.; Baumer, M. *Science* **2010**, *327* (5963), 319.
(51) Calaza, F.; Stacchiola, D.; Neurock, M.; Tysoe, W. T. *J. Am. Chem. Soc.* **2010**, *132* (7), 2202.
(52) Stacchiola, D.; Calaza, F.; Burkholder, L.; Schwabacher, A. W.; Neurock, M.; Tysoe, W. T. *Angew. Chem., Int. Ed.* **2005**, *44* (29), 4572.
(53) Roberts, R. J. M.; Roberts, J. T. In *Surface Reactions*; Madix, R. J., Ed.; Springer-Verlag: Berlin, 1994; p 5.
(54) Zope, B.; Hibbitts, D.; Neurock, M.; Davis, R. J. *Science* **2010**, *330*, 74.
(55) Tanabe, K.; Saito, K. *J. Catal.* **1947**, *35*, 247.
(56) Desai, S. K.; Neurock, M.; Kourtakis, K. *J. Phys. Chem. B* **2002**, *106*, 2559.
(57) Pallassana, V.; Neurock, M. *J. Catal.* **2000**, *191*, 301.
(58) van Santen, R. A.; Neurock, M.; Shetty, S. G. *Chem. Rev.* **2010**, *110* (4), 2005.